Purification of bacterial membrane sensor kinases and biophysical methods for determination of their ligand and inhibitor interactions

Rohanah Hussain*[1], Stephen E. Harding†, Charlotte S. Hughes*‡, Pikyee Ma§, Simon G. Patching§, Shalini Edara§, Giuliano Siligardi*, Peter J.F. Henderson§ and Mary K. Phillips-Jones‡[1]

*Diamond Light Source Ltd., Diamond House, Harwell Science and Innovation Campus, Didcot, Oxfordshire, OX11 0DE, U.K.

†National Centre for Macromolecular Hydrodynamics, University of Nottingham, Sutton Bonington, Leicestershire, LE12 5RD, U.K.

‡Membranes, Membrane Proteins & Peptides Research Group, School of Pharmacy & Biomedical Sciences, University of Central Lancashire, Preston, Lancashire, PR1 2HE, U.K.

§Faculty of Biological Sciences, University of Leeds, Leeds, West Yorkshire, LS2 9JT, U.K.

Abstract

This article reviews current methods for the reliable heterologous overexpression in *Escherichia coli* and purification of milligram quantities of bacterial membrane sensor kinase (MSK) proteins belonging to the two-component signal transduction family of integral membrane proteins. Many of these methods were developed at Leeds alongside Professor Steve Baldwin to whom this review is dedicated. It also reviews two biophysical methods that we have adapted successfully for studies of purified MSKs and other membrane proteins – synchrotron radiation circular dichroism (SRCD) spectroscopy and analytical ultracentrifugation (AUC), both of which are non-immobilization and matrix-free methods that require no labelling strategies. Other techniques such as isothermal titration calorimetry (ITC) also share these features but generally require high concentrations of material. In common with many other biophysical techniques, both of these biophysical methods provide information regarding membrane protein conformation, oligomerization state and ligand binding, but they possess the additional advantage of providing direct assessments of whether ligand binding interactions are accompanied by conformational changes. Therefore, both methods provide a powerful means by which to identify and characterize inhibitor binding and any associated protein conformational changes, thereby contributing valuable information for future drug intervention strategies directed towards bacterial MSKs.

Introduction

It is over two decades since the first emergence of complete genome sequence information for bacteria and higher organisms. Professor Steve Baldwin recognized at a very early stage the huge potential of applying this information for membrane-based drug targeting, urging and encouraging those of us at the University of Leeds (and beyond), to utilize the (then) newly emerging genome databases to discover new membrane protein targets. However, he also realized that there are bottlenecks and technical challenges associated with working with hydrophobic membrane proteins, particularly with regard to their availability in sufficient quantities for fundamental studies including crystallization, NMR spectroscopy, biophysical methods such as isothermal calorimetry, surface plasmon resonance (SPR), fluorescence, analytical ultracentrifugation (AUC), MS and circular dichroism (CD) and for *in vitro* screening to identify ligands and inhibitors. In the case of membrane sensor kinase (MSK) proteins belonging to the bacterial two-component signal transduction family of integral membrane proteins [1–4], insufficient quantities of the intact versions of these membrane proteins has been a contributory factor to the limited crystal structural information available. Here we describe methods (often initially developed alongside Steve and his group working on eukaryotic systems) suitable for the routine production of milligram quantities of purified bacterial MSK proteins. In light of the limited crystal structural data currently available, there has been a need to use biophysical methods to provide structural insights into protein behaviour and to correlate this with functional activities in order to elucidate protein mechanisms and their ligand interactions. Although there are many biophysical techniques available that can be used, in this review we have limited our description to just two of these: synchrotron radiation circular dichroism (SRCD) spectroscopy and AUC, especially in light of recent reviews of some of the other techniques applied to sensor kinases studies such as isothermal titration calorimetry (ITC, which actually requires higher amounts of protein material). The description of AUC includes a range of membrane proteins, rather than MSKs specifically, but highlights the potential

Key words: analytical ultracentrifugation, circular dichroism, histidine kinase, membrane sensor kinase, two-component system.

Abbreviations: AUC, analytical ultracentrifugation; DDM, *n*-dodecyl-β-D-maltoside; GBAP, gelatinase biosynthesis-activating pheromone; IPTG, isopropyl β-D-1-thiogalactopyranoside; ITC, isothermal titration calorimetry; MSK, membrane sensor kinase; SPR, surface plasmon resonance; SRCD, synchrotron radiation circular dichroism.

[1]**Correspondence may be addressed to either of these authors (email MPhillips-Jones@uclan.ac.uk or rohanah.hussain@diamond.ac.uk).**

application of this technique for future studies of MSKs. Both methods are particularly informative regarding membrane protein conformation, oligomerization state and/or ligand binding. As biophysical methods become adapted to studies of membrane (sensor) proteins and more widely used in the future, it is likely that the scientific community in this field will be able to deliver Steve's vision of increased targeting of drugs to membrane proteins, whether it be in eukaryotic or prokaryotic systems.

The histidine protein kinase family of membrane proteins (membrane sensor kinases)

The histidine protein kinase family of proteins (often referred to as MSKs) form part of the two-component signal transduction systems of bacteria, plants and some lower eukaryotes and are principally membrane proteins involved in sensing changes in environmental conditions occurring (usually) on the external side of the membrane. Upon signal perception and environmental ligand binding by a MSK, autophosphorylation occurs followed by phosphotransfer to a partner response regulator protein on the internal side of the membrane, resulting in appropriate responses through changes in gene expression or cell behaviour (motility) (Figure 1A) [1–4]. Sensor kinases are usually integral membrane proteins, possessing as few as two or up to eight transmembrane segments and they have been classified according to the schemes summarized in Figure 1B. They possess conserved regions that permit their relatively easy presumptive identification as histidine protein kinases in the protein–genome databases, but it is much harder to identify the environmental signals and ligands to which they bind because the sensory regions of these proteins, often located within the transmembrane domains, are highly variable. Ligand screening is therefore required which in turn requires production of intact, full-length versions of these proteins that include the hydrophobic membrane-spanning regions within which the sensory binding domains usually reside.

Figure 1 | The histidine protein kinase (or membrane sensor kinase) superfamily

Schematic representation of a bacterial two-component signal transduction system (**A**); classification schemes for the histidine protein kinase superfamily (**B**) [1–4].

A.

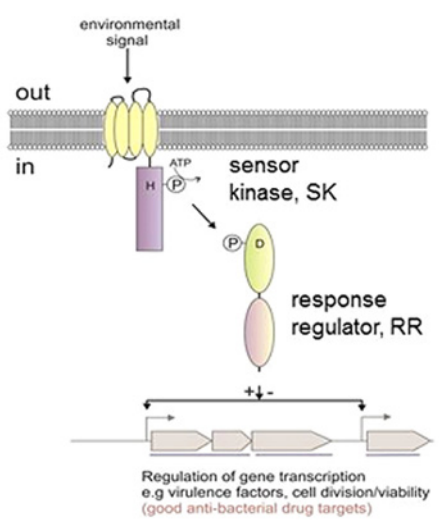

B.

Classification scheme basis	Classes/Groups	Reference
Sequence around the phosphorylated histidine	I-V	[1]
Domain organisation	I and II	[2,3]
Function: domain architecture (membrane topology, number of transmembrane helices, sequential arrangement of the sensory domain within the N-terminal input domain)	I, II and III	[4]

Overexpression and purification of intact His-tagged membrane sensor kinases and their *in vitro* activities

The first report describing the successful heterologous overexpression and purification of any intact bacterial MSK concerned the PrrB (RegB) sensor kinase of the photosynthetic bacterium *Rhodobacter sphaeroides* [5]. Intact PrrB was purified in detergent micelles and shown to retain autophosphorylation, phosphotransfer and phosphatase activities, demonstrating that the activities of the protein were not detectably inhibited by the relatively harsh detergent treatments required for its purification [5]. There was no requirement for protein refolding following detergent treatment. Using the same *in vitro* approach described in [5], phosphorylation assays to screen for and identify the molecular activating ligands involved in the redox-responsive PrrBA pathway revealed small positive effects of chemical reducing agents such as DTT, demonstrating that the purified protein was responsive to its activating ligand and indeed that it was a redox-responsive protein [6]. Since the study of Potter et al. [5], the same approach using intact PrrB protein was used to show that: (1) the redox signal was related to the activity of cbb_3 cytochrome *c* oxidase [7] and (2) an activating redox signal for the RegB homologue in *R. capsulatus* is ubiquinone [8].

To determine whether the *in vitro* approach involving intact membrane proteins described above was reliable for the majority of intact MSKs, we evaluated the systematic cloning, expression, purification and activity assays for the genome complement of 16 MSKs of the hospital-acquired infection agent *Enterococcus faecalis* [9]. The methodology

was adapted to suit this family of membrane proteins which usually possess only 2–8 predicted transmembrane regions together with relatively large soluble domains, making them less hydrophobic than many members of the membrane transport protein family for which the original detergent-based methods were developed [10]. Using PCR-amplified genes cloned into an IPTG (isopropyl β-D-1-thiogalactopyranoside)-inducible pTTQ18His expression plasmid, 15 of the 16 intact sensor kinases were found to be successfully expressed in *E. coli* membranes, 11 out of the 15 proteins retained their autophosphorylation activity in *E. coli* membranes in the absence of test ligand, 14 were successfully solubilized from *E. coli* membranes following solubilization trials and 13 were successfully purified in their intact forms [9]. Of these 13 purified intact proteins, 12 retained autophosphorylation activity suggesting that the methodology was suitable for the majority of intact sensor kinases. Of the 11 proteins shown to be active in *E. coli* membranes above, subsequent solubilization and purification resulted in loss of detectable activity in just one of these proteins (perhaps due to detergent effects), but interestingly a further two proteins that were previously inactive in membranes were now found to be active (albeit weakly in one case) in their purified forms in detergent micelles [9]. It is possible that the environment of the Gram-negative membrane was inhibitory for the activity of these two membrane proteins originating from Gram-positive enterococci and/or that the detergent micellar environment is more favourable for reversion to and retention of active protein conformations in these cases. Figure 2 shows the expression of just one of the *E. faecalis* proteins, FsrC, detected by Western blotting using a $(His)_6$-specific probe for detection of the protein via its engineered C-terminal $(His)_6$-tag (Figure 2). In this example, the membrane fractions were separated by sucrose density gradient centrifugation and although Figure 2 appears to indicate that FsrC locates to both outer and inner membranes in *E. coli*, we suggest that the main location for the majority of these membrane proteins is to the inner membrane only, and that the apparent location to the outer membrane fraction most likely arises through incomplete separation of inner and outer membranes in the sucrose gradients which can be technically challenging.

Conditions for optimized expression were identified for many of the proteins by trialling different growth media (e.g. Luria–Bertani, 2TY (also known as 2YT) and M9 minimal media, [12]), induction conditions (e.g. IPTG inducer concentration) and incubation time post-induction prior to cell harvesting. Comparisons of the various conditions tested were made using the SDS/PAGE and Western blotting methods shown in Figure 2. Protein purification utilizing inner membrane preparations derived from *E. coli* BL21 [DE3] cells expressing each protein employed the nickel affinity purification methods described previously [9,10,13]. Optimization of detergent type and concentration is also important with respect to compatibility with the planned downstream experimental technique(s) [14–16]. Following solubilization of membrane proteins using 1% detergent (usually *n*-dodecyl-β-D-maltoside, DDM, for the enterococcal MSKs), all buffers in the subsequent nickel affinity purification steps contained 0.05% detergent to maintain protein solubility. Figure 3 shows samples of fractions obtained during the purification procedure for two of the enterococcal proteins, FsrC and EF1051. Following the optimizations outlined in [9], most of the MSKs could be purified to >95% purity for subsequent biophysical analyses or crystallization trials. Verification that proteins were produced intact was obtained by MS and/or Western blotting for detection of the engineered C-terminal His_6-tag (Figures 2 and 3), and N-terminal sequencing.

Lower concentrations of detergents (e.g. 0.02–0.025% DDM), have been used with some of the *E. faecalis* V583 proteins from our laboratory [17,18] but longer incubation periods were required before data collection during downstream biophysical methods such as CD spectroscopy. Buffer conditions are protein-specific, so the composition will vary for each sensor kinase. Table 1 provides an example of buffer optimization for the VanS MSK involved in A-type vancomycin resistance in *E. faecium*. Unlike other enterococcal MSK proteins [9], intact VanS was found to be highly sensitive during buffer screens (Table 1). The final buffer composition is often a case of trial-and-error. Factors such as pH, salt, buffering system and final concentration of the

Table 1 | Final exchange buffer conditions used for preparations of VanS and the results of the different buffer choices

*Precipitation was also observed using: 50 mM Tris/HCl pH 7.5, 100 mM NaCl, 0.05% DDM; 10 mM Tris/HCl pH 7.5, 25 mM NaCl, 0.05% DDM; 10 mM Tris/HCl pH 7.5, 100 mM NaCl, 0.05% DDM; 10 mM Tris/HCl pH 7.5, 300 mM NaCl, 0.05% DDM; 50 mM Tris/HCl pH 7.5, 300 mM NaCl, 0.05% DDM; 10 mM Tris/HCl pH 7.5, 5% glycerol (v/v), 100 mM NaCl, 0.05% DDM, 2 mM mercaptoethanol; 25 mM Tris/HCl pH 7.5, 5% glycerol (v/v), 100 mM NaCl, 0.05% DDM, 2 mM mercaptoethanol; 10 mM NaPi pH 7.2, 100 mM NaCl, 0.05% DDM; 10 mM NaPi pH 7.2, 25 mM NaCl, 0.05% DDM and 50 mM NaPi pH 7.2, 25 mM NaCl, 0.05% DDM.

Exchange buffer (BE)	Visible appearance
50 mM NaPi pH 7.2, 0.05% DDM, 100 mM NaCl See * for other exchange buffers causing VanS precipitation	Precipitated after buffer exchange (BE) (but before concentrating); other batches showed no precipitation during concentration stages, but precipitated overnight post-concentration at 4°C
10 mM HEPES pH 7.9, 20% glucose, 0.025% DDM	Remained clear and colourless. Stable at 4°C for over 2 months
10 mM HEPES pH 7.9, 0.05% DDM, 10% glycerol, 100 mM NaCl	Remained clear and colourless. Stable at 4°C for over 2 months
10 mM HEPES pH 7.9, 0.025% DDM, 20% glycerol	Clear. Stable for over 2 months at 4°C

Figure 2 | **Overexpression in *E. coli* of the intact His-tagged FsrC (EF1820) MSK of *E. faecalis***

SDS/PAGE (left) and Western blot (right) analyses of membrane fractions of *E. coli* BL21[DE3] cells expressing FsrC. Mixed *E. coli* membranes were prepared from *E. coli* BL21[DE3]/pTTQ18FsrC-His_6 cultured in Luria–Bertani medium containing 20 mM glycerol and 100 μg/ml carbenicillin and induced with 0.5 mM IPTG. Cultures were harvested 3 h after IPTG induction. The inner and outer membranes were at least partially separated on 25–55 % sucrose gradients, extracted and analysed by SDS/PAGE and Western blotting using an INDIA His probe [9]. M, molecular mass markers. Recombinant FsrC has a predicted molecular mass of 53.4 kDa; anomalous migration by membrane proteins in SDS/PAGE is well documented. The arrow indicates the position of FsrC (EF1820). (Data from [11]: Ma, P. (2010) Structure–Activity Relationships of Membrane Proteins: The NCS1 Family of Transporters and Sensor Kinases of Two-Component Systems. Ph.D. thesis, University of Leeds, UK.).

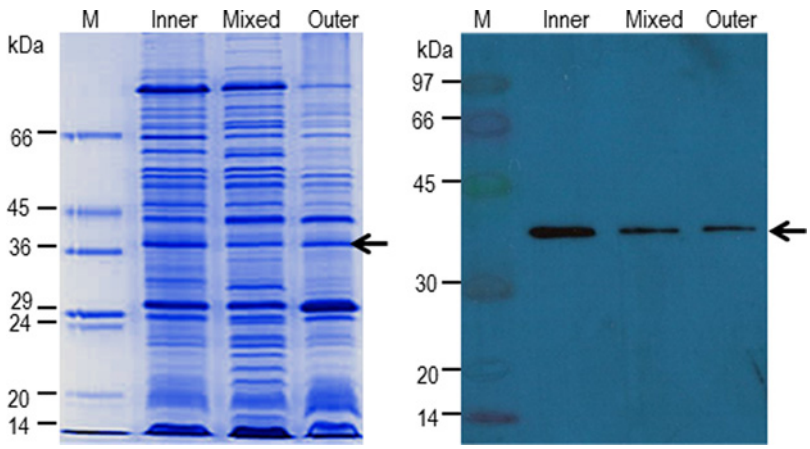

Figure 3 | **Purification of His-tagged FsrC (EF1820) (A) and EF1051 (B) MSKs of *E. faecalis* V583**

Both proteins were overexpressed in inner membranes of *E. coli* BL21[DE3] cells expressing pTTQ18FsrC-His_6 or pTTQ18EF1051-His_6, respectively, solubilized using 1 % DDM and subjected to nickel chelate affinity chromatography as described in [9]. Fractions (15 μg) from the purification and chromatography steps and the final eluted purified proteins (5 μg) were analysed by SDS/PAGE (**A** and **B**) and rightmost (**B**) by Western blot using an INDIA His probe for detection of the C-terminal His_6 tag of EF1051 [9]. M, molecular mass markers. Arrows denote the positions of purified (**A**) FsrC (expected molecular mass of 53.4 kDa) or (**B**) EF1051 (60.2 kDa). Anomalous migration by membrane proteins in SDS/PAGE is well documented. (Data from [11]: Ma, P. (2010) Structure–Activity Relationships of Membrane Proteins: The NCS1 Family of Transporters and Sensor Kinases of Two-Component Systems. Ph.D. thesis, University of Leeds, UK.).

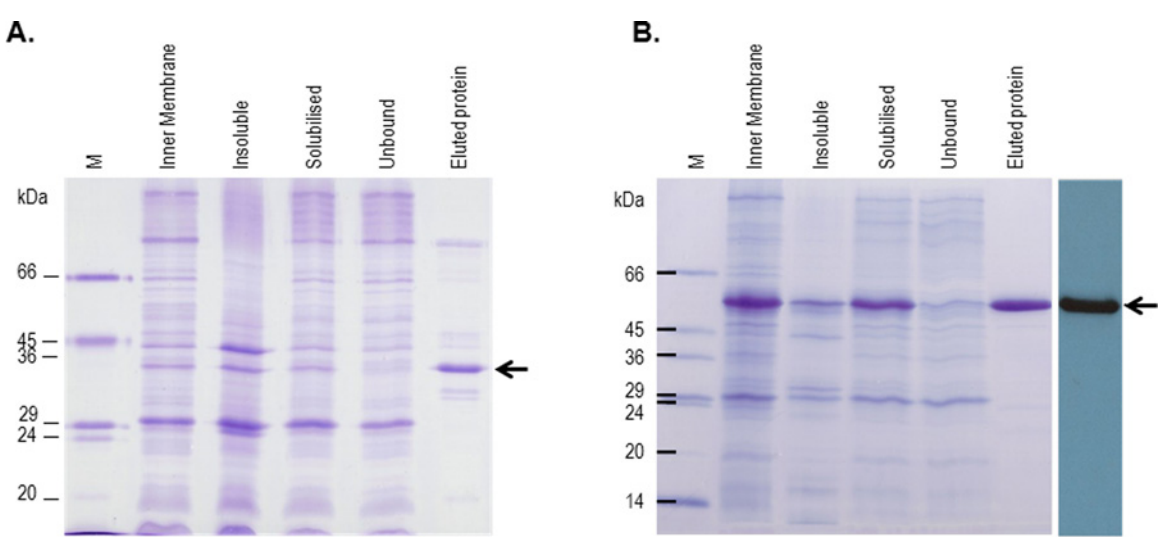

protein need to be considered. The large soluble portions of histidine sensor kinases may allow for greater flexibility in the purification process than traditional multi-transmembrane proteins, but, as in the case of VanS, the buffer used for one experimental system may not be appropriate for another.

Two examples of the effects of buffer composition and detergent concentrations on the activities of intact sensor kinases are shown in Figure 4. Interestingly, for both EF1051 and VanS purified proteins, the presence of 0.05 % DDM was inhibitory to autophosphorylation activities and to the levels of phosphorylation attained in the assays (Figure 4). We observed this previously for other purified MSKs such as VicK and found that activity was restorable upon adjustment of DDM concentrations from >0.05 to 0.025 %. Therefore, to obtain active proteins, it is advisable to reduce detergent concentrations as low as possible following the membrane solubilization step, to just above the CMC value [which is approximately 0.17 mM (0.00 867 %) for DDM]. We propose that the reduced activity levels observed in the presence of detergent may be attributable to a reduced ability of the purified proteins to dimerize in the presence of detergent. Until recently, the classic model for the autophosphorylation mechanism of MSKs proposes formation of dimers to facilitate the transphosphorylation of both conserved histidine residues in each monomer [19–21]. However, recent alternative models propose monomeric phosphorylation and regulation of signal transduction [22]. Although both models may be correct for different sensors, our results of reversible detergent inhibition of sensor activities are consistent with a role for dimerization in the phosphorylation mechanism and hence with the classic model, at least in the case of the sensors we have investigated to date.

Use of circular dichroism spectroscopy for conformational analysis and ligand binding studies of the purified FsrC and CrdS membrane sensor kinase proteins

Protein–ligand binding interactions can be assessed by a variety of techniques such as ITC, SPR, fluorescence, AUC, MS, NMR including magic-angle NMR, SAXS and CD. For systems in solution where one of the interacting molecules is not immobilized or labelled, the techniques are limited to ITC, AUC and CD. CD can assess directly whether the binding interactions are accompanied by conformational changes.

To measure a CD spectrum the molecule has to be chiral and possess at least a chromophore group absorbing light in the wavelength region investigated. For proteins, the far-UV region (185–260 nm) is characteristic of backbone folding whereas the near-UV region (260–330 nm) characterizes the local tertiary structure of the aromatic side-chain residues such as tryptophan, tyrosine and phenylalanine and dihedral angles of the disulfide bonds [23]. CD, defined as the differential absorption of left and right circularly polarized light for a chiral molecule, follows the Beer's law, $A = \varepsilon Cl$, in which A is the absorbance (no unit), ε the molar absorption coefficient ($M^{-1}\cdot cm^{-1}$), C is the concentration in molarity (M) and l the cell pathlength in cm. If there are no concentration effects, the CD spectrum of a protein solution of 1 mg/ml in a 0.1 mm pathlength cell, for example, will be superimposable on to that for the 10-fold diluted solution (0.1 mg/ml) in a 10-fold longer pathlength cell of 1 mm.

The golden rules to measure a good signal-to-noise CD spectrum of protein solutions in the far-UV region characteristic of the proteins' folding can be summarized as follows:

(i) Prepare protein concentrations in the range of 0.3–0.5 mg/ml for measurement with a fused silica cell of 0.02 cm pathlength. In this manner, the ideal UV absorbance of the solution should not be lower than 0.5 nor greater than 1.5. Ideally it should be approximately 0.8.

(ii) With modern CD instruments, the far-UV wavelength range that can be scanned with a 0.02 cm pathlength cell is from 260 to 185 nm for proteins in pure water. However, more often than not, protein stability requires the presence of high sodium chloride concentrations. Chloride anions are not optically transparent below 200 nm, therefore for lower wavelength measurements narrower pathlengths are needed with also increased protein concentrations following Beer's Law. Guidelines for solvent/buffer cut-off using B23 beamline are reported in Table 1. SRCD beamlines can penetrate by 5–10 nm the cut off of the solvents/buffers encountered with bench top instruments, however, any CD band observed below 170 nm should be treated as artefactual due to noise.

(iii) The majority of membrane proteins are suspended in DDM detergent which is transparent in the far-UV region. Hence CD measurement is not impaired. However, detergents such as Sarkosyl, typically used at a concentration of 0.5 % for suspension of membrane proteins, is best avoided as it has an absorption in the far-UV with a cut-off at ∼ 220 nm in a standard 0.02 cm pathlength cell, preventing any useful data important for the determination of secondary structure to be collected. Sarkosyl can be used however, if the concentration of the proteins are kept high (above 5 mg/ml). In this case a shorter pathlength cell can be used (such as 20 micron or less), while maintaining a good signal-to-noise ratio in the CD signal.

(iv) It is also good practice for membrane proteins suspended in detergent to be incubated for sufficient equilibration time to allow the protein to stabilize in the detergent buffer condition.

CD relies on detectable spectral differences between the observed spectrum of the protein–ligand mixture at (x:y) molar ratio and that calculated from the sum of the spectra of the protein at (x) molar ratio and ligand at (y) molar ratio. For achiral ligands, the comparison is facilitated by the fact

Figure 4 | Examples of the importance of buffer composition and detergent concentration on the activities of purified intact MSKs, exampled by: (A) *E. faecalis* EF1051 and (B) *E. faecium* A-type VanS

Intact proteins were solubilized from *E. coli* BL21[DE3]/pTTQ18EF1051-His_6 or *E. coli* BL21[DE3]/pTTQ18VanS-His_6 inner membranes using 1% DDM. Purification was performed in the presence or absence of additional DDM in Tris-based or HEPES-based buffer systems (**A**):10 mM Tris/HCl pH 7.6 or 10 mM HEPES pH 7.6; (**B**) 10 mM HEPES pH 7.9. Autophosphorylation activities of purified proteins were assayed using radiolabelled ATP as described in [5] and [9], with samples withdrawn to stop buffer: (**A**) at 2 and 15 min intervals or (**B**) at 30 min following ATP addition. Autoradiographs are shown. The arrows indicate the positions of the phosphorylated proteins (EF1051 data from [11]: Ma, P. (2010) Structure–Activity Relationships of Membrane Proteins: The NCS1 Family of Transporters and Sensor Kinases of Two-Component Systems. Ph.D. thesis, University of Leeds, UK).

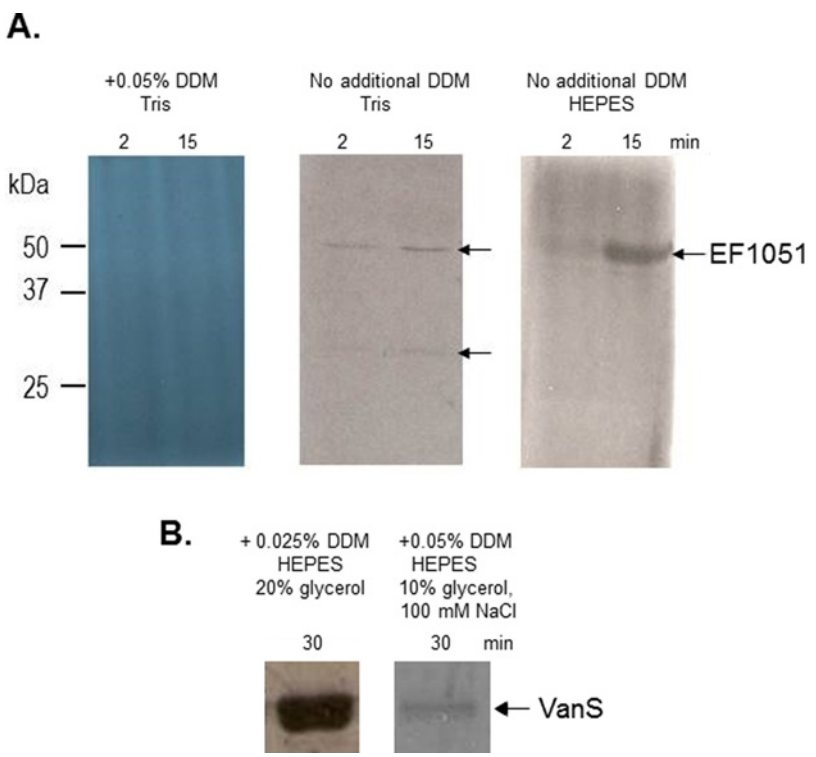

that upon binding, the ligand chromophore will acquire an induced CD upon binding to a protein site that is chiral. In this case the detection of any induced CD, which is any spectral difference from that of the protein alone, must reflect the presence of a bound species as the free achiral form is devoid of any CD signal [23–26]. However, for ligands having weak or no UV chromophore groups, such as sugars, lipids and unordered peptides, the lack of any CD spectral change upon ligand addition does not necessarily signify that there are no binding interactions. Also, the ligand might actually bind but too far from the aromatic side chains of the peptide/protein to cause any detectable secondary structure conformational change between the host protein and ligand molecule, so no spectral change is detected from that of the host protein alone. For these reasons, the protein UV denaturation assay using beamline B23 has been developed and is now one of the facilities available for users at the Diamond B23 beamline (Figures 5 and 6) [27,28]. High UV photon flux at B23 has been used to distinguish qualitatively binding of ligands to proteins such as non-steroidal anti-inflammatory drugs to serum albumin, though this is not a membrane protein [27]. UV denaturation has also been used to discriminate the effects of different excipients (detergents, salts, buffers etc.) of a drug formulation, on peptide hormones such as vasoactive peptide VIP which binds to a GPCR (G protein-coupled receptor) [29] and on antibodies such as Cetuximab which are inhibitors of the epidermal growth factor receptor (EGFR) transmembrane protein [30,31]. These types of measurements are easy to carry out as they require only repeated consecutive scans of protein samples with and without ligands. Plotting the rates of such photo-denaturation decays enables a qualitative assessment of binding interactions as well as of photostability [32,33].

Binding studies using CD titration methods is even more challenging for membrane proteins than cytosolic soluble proteins. A common limitation encountered with membrane proteins is that they are often expressed in rather small quantities. At the B23 beamline, the highly collimated micro-beam (0.3×0.5 mm) is enabling the use

Figure 5 | Optical layout of CD spectrometer and Diamond B23 SRCD beamline

(**Top**) Optical layout of CD spectropolarimeter: S, light source (arc Xe lamp for bench-top); M, monochromator; P, polarizer; PEM, photo elastic modulator; LCP and RCP, left and right circularly polarized light, sample and detector. (**Middle**) Optical layout of Diamond B23 beamline. The light source is originated tangentially from Diamond synchrotron bending magnet. In the experimental room, the orange box contains the optical elements illustrated in the top figure. (**Bottom**) Photo of B23 experimental room showing two end-stations: module A dedicated for CD imaging, variable temperature studies (cryogenic to high temperatures) and HT-CD measurements, and module B for standard CD measurements though exploiting the higher photon flux of B23 pushing the vacuum ultraviolet (VUV) wavelength range limit.

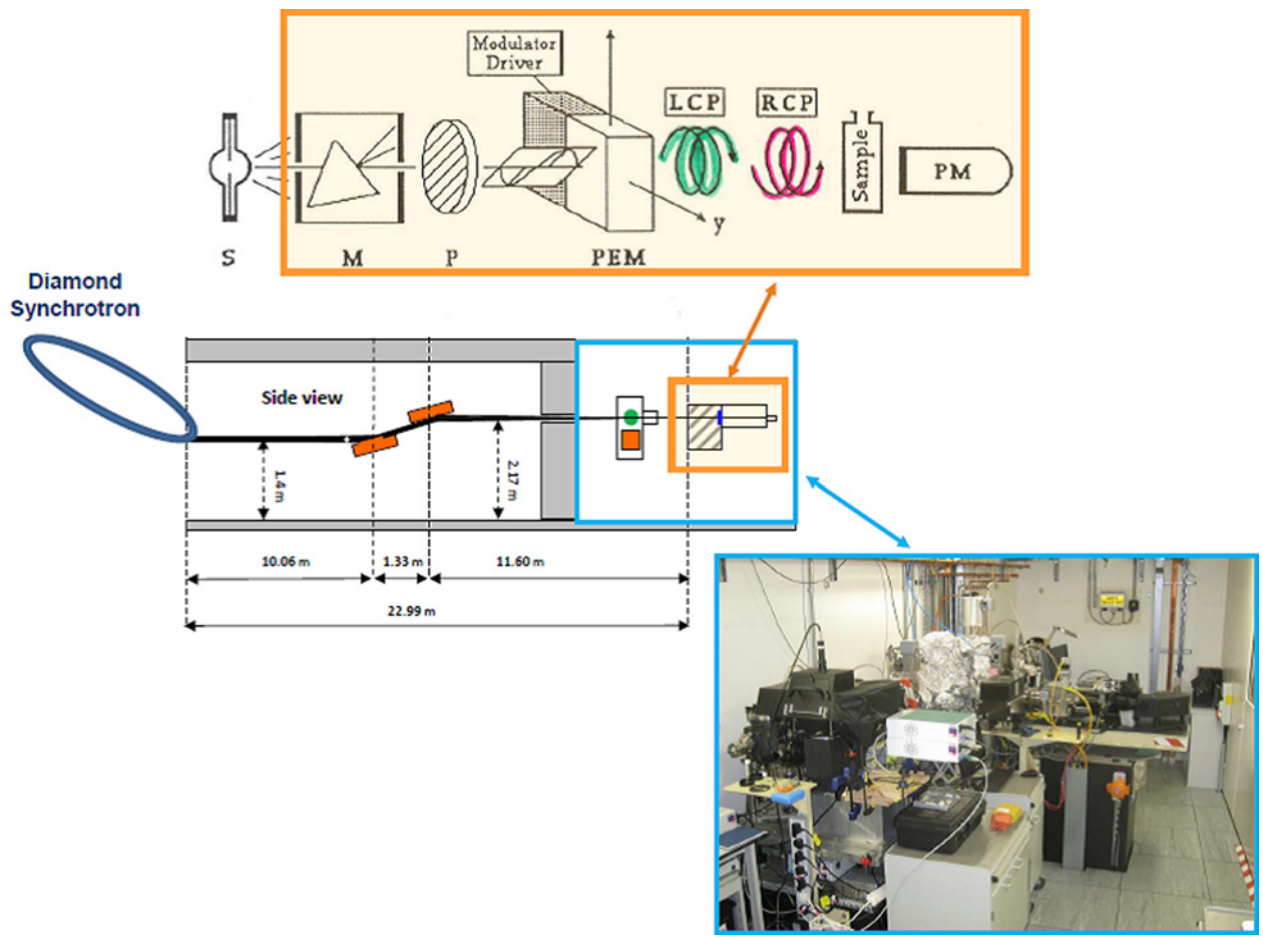

of small aperture cuvette cells of low volume capacity (a few μl to approximately 50 μl for 0.01–1 cm pathlengths respectively) to measure the SRCD spectra of precious and scarce membrane proteins [17,34–37]. Secondary structure estimations can be carried out at Diamond using CDApps [38] with a suitable algorithm such as CONTINLL [39].

Several examples of sensor kinases are discussed below to illustrate the approach developed and used successfully by CD and SRCD spectroscopy at beamline B23.

FsrC from *E. faecalis* is a MSK which showed very little conformational change in secondary structure upon addition of its ligand gelatinase biosynthesis-activating pheromone (GBAP) (Figure 7A). However the local tertiary structure of FsrC showed significant changes when GBAP was added indicating involvement of aromatic residues binding to GBAP (Figure 7B). Quantitative studies revealed the ligand GBAP to have an affinity (K_d value) for FsrC of 2 μM monitored at a single wavelength (277 nm) (Figure 7C). Further competitive binding studies with another ligand, inhibitor siamycin I, showed that siamycin I did not compete with GBAP and that aromatic side-chain residues were affected by the interaction with both ligands (Figure 7B) [17,34].

Batch differences can occur during protein production, even though the expression and purification conditions are kept the same and these must be considered as a factor during experimental design. This consideration emerged in our studies of FsrC which showed little conformational difference at the secondary structural level batch-to-batch, but did exhibit local tertiary structural changes (Figure 8) [17,34]. In this example, even though the different batches of FsrC exhibited some structural differences, the kinase activity was

Figure 6 | Comparisons of SRCD and bench-top CD in the far-UV region with small aperture cell

(**Top**) CD spectra of 8 μM fatty acid-free human serum albumin (HSA) in water recorded in a Suprasil quartz capillary (insert right) of normalized 0.02 cm pathlength (equivalent aperture 1.24 mm (w) × 1.5 mm (h) irradiated with a light beam of approximately 0.5 mm diameter) with B23 Module B (black line) and bench-top CD instrument (Chirascan, Applied Photophysics, UK) (red) SRCD spectrum using cylindrical cell (insert right) of 0.02 cm pathlength was measured with Module B (green dotted). Each spectrum was an average of 4 scans with total acquisition time approximately 9 min. (**Bottom**) High voltage of photomultiplier (PMTs) detectors of Module B (black) and bench-top instrument (red) showing a cut-off below 200 nm, which led to a noisier CD spectrum. All spectra were measured with bandwidth of approximately 1 nm.

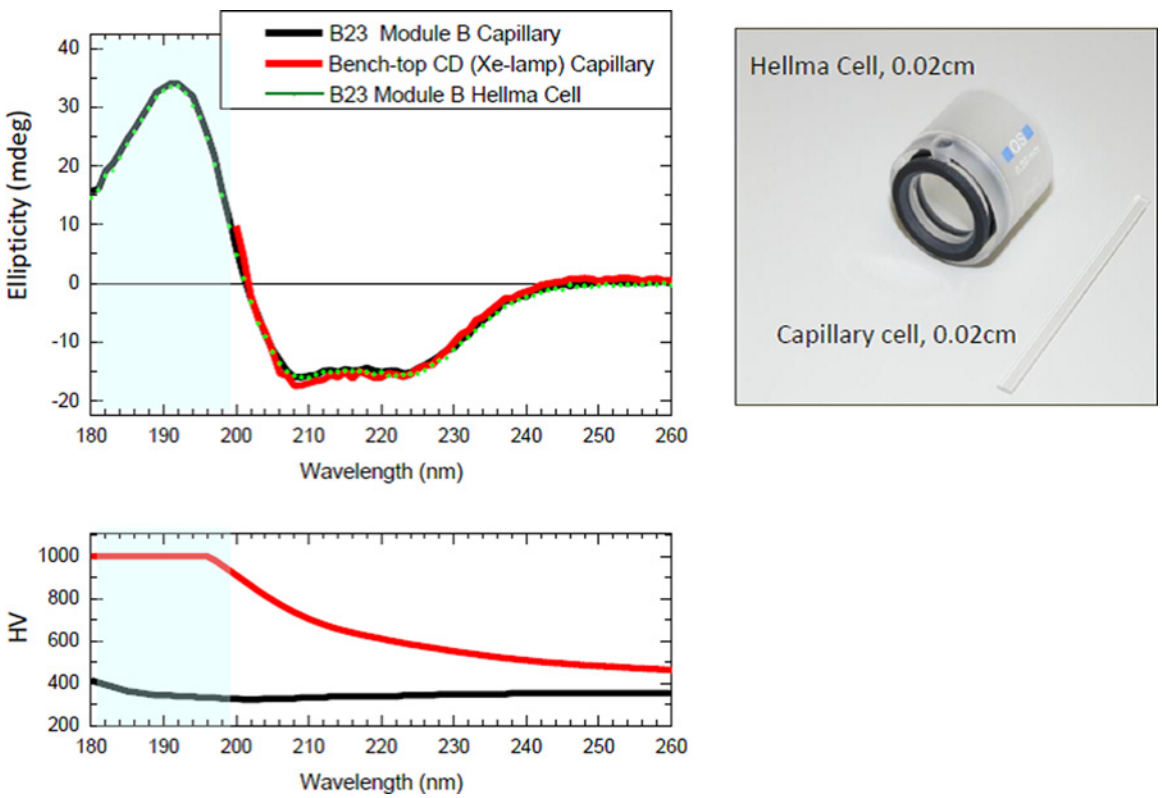

not affected nor was the binding to the GBAP ligand. These findings may highlight the impacts that different protein batches could have on activity assays or other functional studies. Therefore CD spectroscopy may provide a useful tool for confirming consistency among protein batches with regard to conformation and other properties prior to activity assays and other functional studies [31].

Mutant studies

Conformational differences between wild type and mutant proteins may be identified using CD spectroscopy [40–42]. For example, such an approach was used in studies of *Myxococcus xanthus* CrdS, which is a member of the HisKA subfamily of bacterial sensor kinases and is required for regulation of spore formation in response to environmental stress. The kinase and phosphatase activities of a collection of CrdS mutant proteins were evaluated by Willett and Kirby [40]. In addition, using far-UV CD spectroscopy, they also demonstrated that all mutant and wild-type CrdS proteins were predominantly α-helical with distinctive double minima at approximately 210 and 222 nm (Figure 9) (a feature typical of α-helical membrane proteins, which also characteristically exhibit a positive maximum at ~190 nm that is twice in absolute intensity to that at 210 nm, not shown). Notably all strains (mutant and wild type) were indistinguishable in terms of their secondary structural conformations, suggesting that any activity changes in the mutants were not accompanied by (or due to) changes in the secondary structural conformations of the proteins (Figure 9) [40]. Here in this example the limitations of the benchtop instrument emerge as there is a loss of signal in the far-UV region 180–200 nm which limits the information required to estimate correctly the secondary structure content of the protein using the well-established algorithms such as Continll, Selcon and Cdsstr which have a requirement for data from 190 nm upwards.

Use of analytical ultracentrifugation for oligomeric state analysis and ligand binding studies of membrane proteins

Like CD, AUC is another – and complementary – method for assessing protein–ligand interactions [43] and

Figure 7 | Binding interaction properties of FsrC membrane protein determined using the B23 beamline for SRCD spectroscopy (figures A–C are redrawn from [17]: Patching, S.G., Edara, S, Ma, P., Nakayama, J., Hussain, R., Siligardi, G. and Phillips-Jones, M.K. (2012) Interactions of the intact FsrC membrane histidine kinase with its pheromone ligand GBAP revealed through synchrotron radiation circular dichroism. Biochim. Biophys. Acta Biomembr. 1818, 1595–1602 and [34]: Phillips-Jones, M.K., Patching, S.G., Edara, S., Nakayama, J., Hussain, R. and Siligardi, G. (2013) Interactions of the intact FsrC membrane histidine kinase with the tricyclic peptide siamycin I revealed through synchrotron radiation circular dichroism. Phys. Chem. Chem. Phys. 15, 444–447)

(**A**) Far-UV SRCD spectra and (**B**) near-UV SRCD spectra of FsrC membrane protein with: siamycin I (dashed black line), siamycin I and GBAP (dotted line), GBAP (solid black line) or no ligand (grey line). (**C**) The fitting of the GBAP SRCD titration into FsrC protein using a non-linear regression analysis. The K_d value calculated from CD data was 2 μM. The unique micro-collimated beam of Diamond's B23 beamline enabled the measurements to be carried out using small amounts of protein in small volume capacity cells (50–100 μl) of 1 cm pathlength unattainable with bench-top CD instruments. Data from [17]: Patching, S.G., Edara, S, Ma, P., Nakayama, J., Hussain, R., Siligardi, G. and Phillips-Jones, M.K. (2012) Interactions of the intact FsrC membrane histidine kinase with its pheromone ligand GBAP revealed through synchrotron radiation circular dichroism. Biochim. Biophys. Acta Biomembr. **1818**, 1595–1602 and [34]: Phillips-Jones, M.K., Patching, S.G., Edara, S., Nakayama, J., Hussain, R. and Siligardi, G. (2013) Interactions of the intact FsrC membrane histidine kinase with the tricyclic peptide siamycin I revealed through synchrotron radiation circular dichroism. Phys. Chem. Chem. Phys. **15**, 444–447.

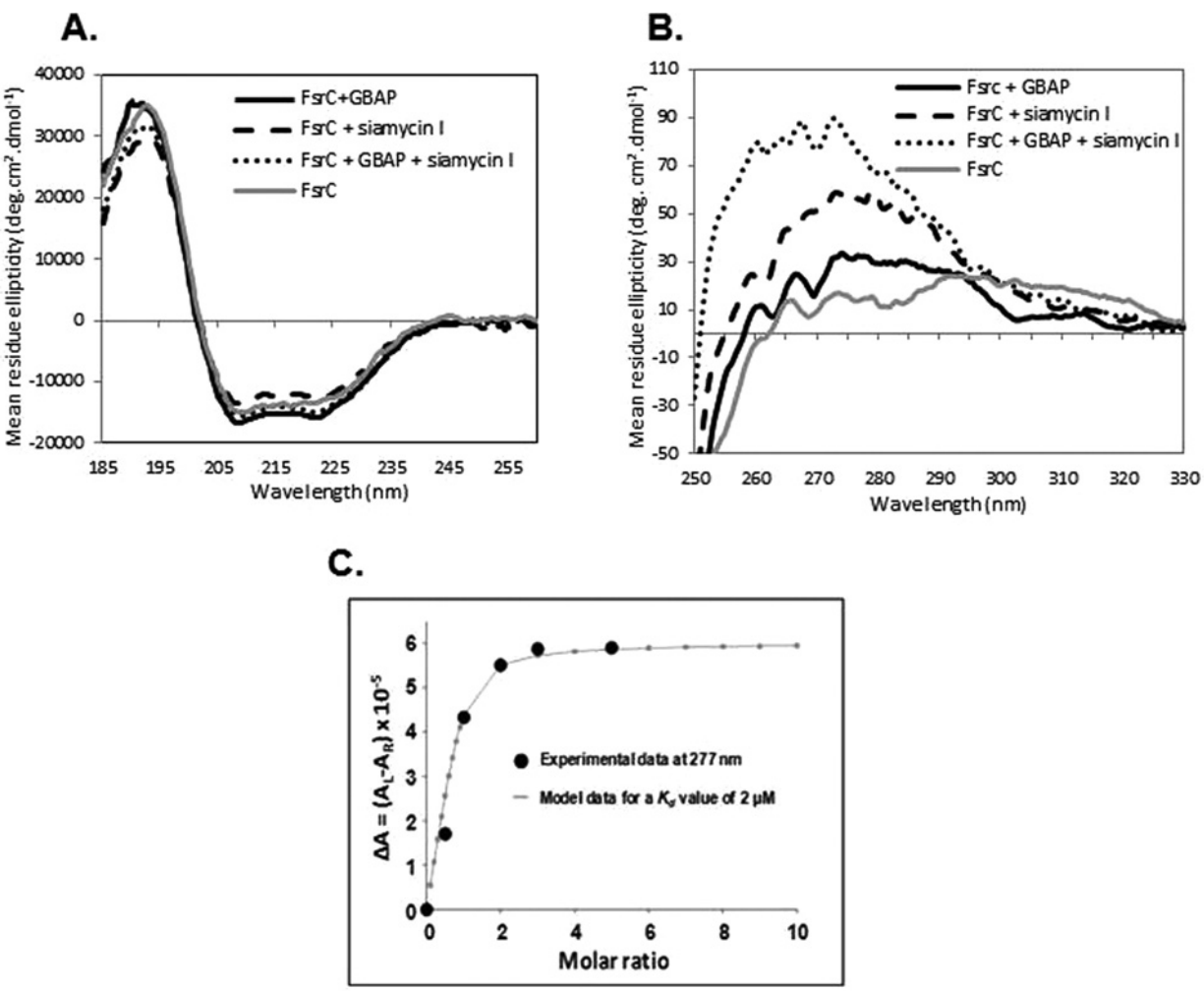

also self-association reactions [44] without the need for immobilization, labelling or an assumed inert separation matrix. It can also yield conformation information, not so much at the secondary structural level that CD can provide but at the overall gross conformational level (ellipsoids and bead models), particularly when used in conjunction with data from other techniques [45]. Although insofar as we know, it has yet to be applied to kinase-based systems, it

Figure 8 | **Two different batches of intact FsrC membrane protein**

(**A**) Far-UV CD spectra of FsrC showing little conformational difference. (**B**) Near-UV CD spectra showing differences in the local tertiary structure of FsrC.

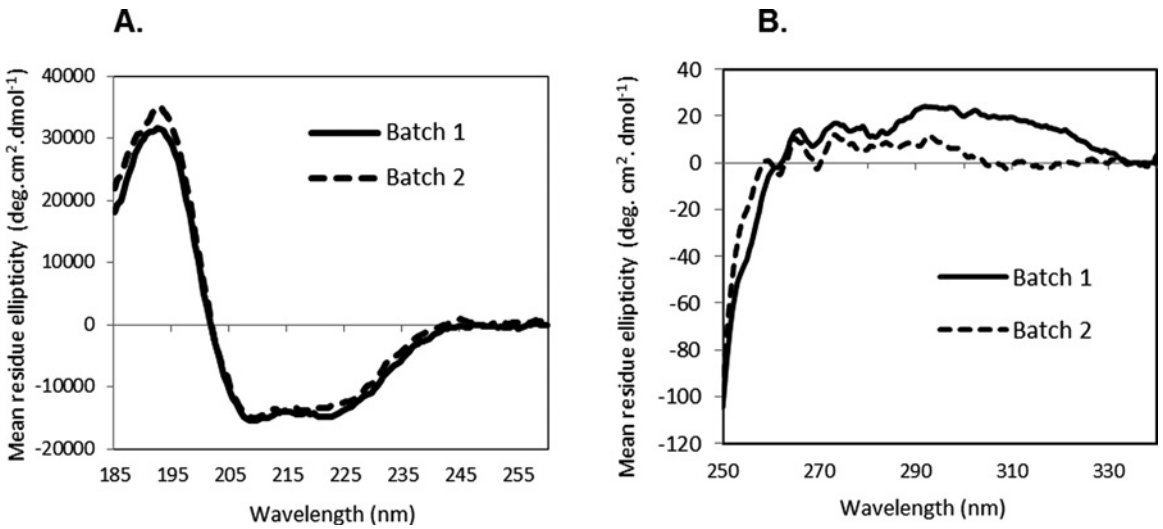

Figure 9 | **The secondary structural conformations of CrdS and its mutant derivatives**

Far-UV CD spectra of CrdS wild type and mutant proteins (redrawn from [40]: Willett, J.W. and Kirby, J.R. (2012) Genetic and biochemical dissection of a HisKA domain identifies residues required exclusively for kinase and phosphatase activities. PLoS Genet. **8**, e1003084). WT denotes wild type.

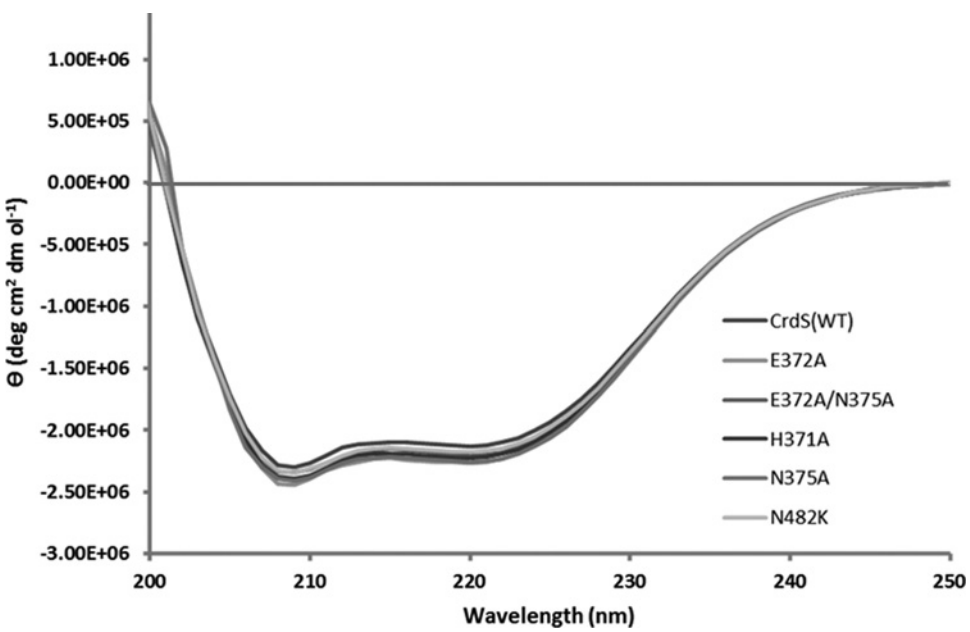

has been applied to a number of other membrane-based systems.

In sedimentation velocity the (weight average) sedimentation coefficient, *s* (ratio of the sedimentation rate to the centrifugal field) and distribution of sedimentation coefficients is measured – from the change of the concentration distribution in an ultracentrifuge cell with time. A popular algorithm for performing the transformation is SEDFIT [46] which provides *s*, the sedimentation coefficient distribution – *g*(*s*) versus *s*, and also the distribution corrected for diffusion broadening, *c*(*s*) versus *s*. Since the sedimentation coefficient distributions depend on conformation as well as

molar mass (in g/mol, or equivalently 'molecular mass' in Da), it is possible to transform distributions to molecular mass distributions for monodisperse solutions or mixtures with a small number of components. For more polydisperse systems the transformation is still possible using additional information from sedimentation equilibrium or light scattering [47]. For self-associating or interacting systems reversibility can be checked by running at a range of loading concentrations. For ligand binding studies, co-sedimentation (looking for materials sedimenting at the same rates), can be used very powerfully [43]. In sedimentation equilibrium [48] the ultracentrifuge is run at lower rotational speeds so that the back forces due to diffusion become comparable with the centrifugal forces. At equilibrium, frictional/conformational effects are eliminated and the optical records give a direct measure of molar mass/oligomeric states and association constants, again at a range of concentrations [44]. The primary information is the weight average molar mass, M_w. From the way M_w changes with loading concentration, or the way $M_w(r)$ versus $c(r)$ varies within a run – or by modelling the $c(r)$ versus r distributions directly – it is possible to ascertain the stoichiometry and reversibility of self-associative or heterologous interactions. Popular algorithms are SEDFIT-MSTAR [48] for determining average molar masses, MULTISIG [49] for distributions and SEDPHAT [50] for analysis of interacting systems.

Non-ideality effects are taken care of by working at low concentration (<0.5 mg/ml) or extrapolation to zero concentration. With membrane systems, if detergents are required for solubilization, knowledge of the extent of binding of the detergent to the protein is needed (from, e.g. ^{14}C measurements [51]) as well as the partial specific volume of the protein (this can be obtained from density measurements – see [44,52]).

Figure 10 | Sedimentation equilibrium concentration for the cytoplasmic domain of the Band 3 transporter

Protein concentration (expressed in terms of UV absorbance at 280 nm in a 12 mm optical path length cell) versus the radial displacement at a given position in the cell. Equilibrium speed 10000 rpm (8000 ***g***, depending on radial position), temperature 20.0 °C, loading concentration $c = 0.18$ mg/ml. The line fitted (residuals fit also shown above) is for an ideal reversible dimerization with $K_d = (2.8 \pm 0.5)$ μM (from [53]: Cölfen, H., Harding, S.E., Boulter, J.M. and Watts, A. (1996). Hydrodynamic examination of the dimeric cytoplasmic domain of the human erythrocyte anion transporter, band 3. Biophys. J. **71**, 1611–1615).

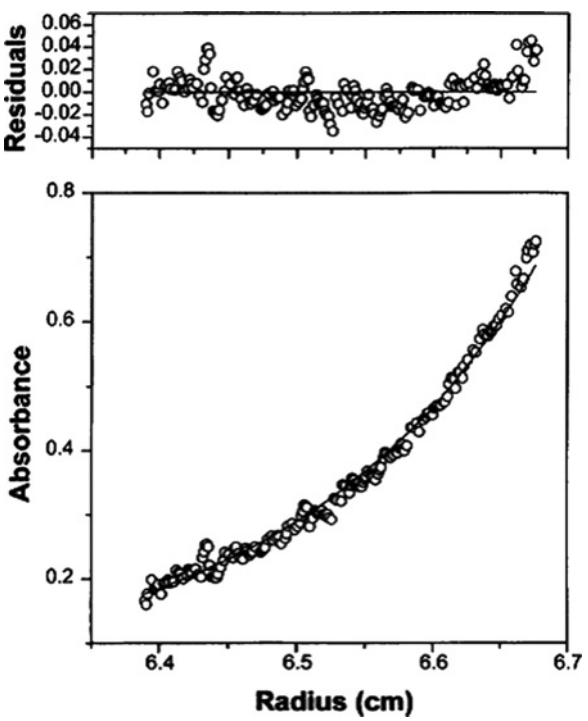

Band 3 protein

One system which has been extensively studied is the human erythrocyte anion transporter Band 3 [53–55]. Sedimentation equilibrium studies [53], on the aqueous soluble cytoplasmic domain ($M \sim 40$ kDa) revealed that it reversibly dimerized to a moderate degree with a K_d of (2.8 ± 0.5) μM (Figure 10) and from estimation of the frictional ratio from sedimentation velocity it was clear the protein was elongated (axial ratio $a/b \sim 10{:}1$). By contrast the transmembrane domain [54], solubilized in C12E8 ($M \sim 55$ kDa) is a stable dimer with no sign of dissociation (at least down to 0.1 mg/ml), and has a more spheroidal conformation in solution ($a/b \sim 3{:}1$), consistent with 2D crystal images from electron microscopy. Finally the intact Band 3 protein was studied (solubilized in reduced Triton X-100) and showed a more complex dimer–tetramer–hexamer equilibrium [55].

In similar work, a membrane fusion protein known as **EmrA**, and in particular fragment EmrA(49–390) has been studied [56]. This protein is part of the multidrug resistance pump of Gram-negative bacteria. Sedimentation equilibrium showed the molar mass was 41 kDa consistent with the monomeric value of 39.6 kDa from the sequence. Sedimentation velocity showed the molecule to be highly elongated ($a/b \sim 12$) consistent with the predicted structure of a β-barrel extended to a long helical coil. In other work the **CD2–CD48** T-cell recognition system has been studied showing a weak heterologous interaction between the two components [57], whereas co-sedimentation has been used for example to show that cytochrome *c* peroxidase binding to both cytochrome 550 and pseudoazurin appears to be competitive rather than co-operative [58].

Concluding remarks

In this review we highlight some of the recent successes for the reliable production of microgram and milligram quantities of purified intact MSKs from enterococci and for their biophysical characterization and ligand screening. A high rate of success in production of the genome complement

of enterococcal sensor kinases proteins was achieved using a pTTQ18-based plasmid expressed in *E. coli* BL21 [DE3], perhaps attributable to the large soluble portions present in these proteins. Nonetheless, they are also integral membrane proteins, requiring detergents for their solubilization from host membranes prior to purification. DDM proved to be a particularly suitable detergent with accompanying retention (in all but one case) of activity post-purification. A very high proportion of enterococcal MSKs were therefore successfully expressed in *E. coli*, solubilized from inner membranes using DDM detergent and purified in active intact forms, as examplified in this review by EF1820 (FsrC), EF1051 and type A VanS.

For ligand studies the use of SRCD spectroscopy and AUC are reviewed here, both of which are non-immobilization and matrix-free methods that require no labelling strategies and yet can provide information on membrane protein conformation, oligomerization state and ligand binding, with an additional advantage of providing direct assessments of whether ligand binding interactions are accompanied by conformational changes. SRCD studies of FsrC resulted in the first quantitative binding data on ligand binding for any membrane protein. This was a relatively recent successful development and applied use of CD spectroscopy. But it also remains a powerful tool for verifying secondary structural integrity for soluble and membrane proteins alike, including sensor kinases such as CrdS and its mutant forms. Although AUC has not yet, to our knowledge, been applied to studies of MSKs specifically, it is clearly a very suitable technique for studies of this membrane protein family having already been successfully used to investigate other membrane and membrane protein-interacting proteins such as Band 3, EmrA, CD2–CD48 and cytochrome *c* peroxidase with regard to their oligomerization state, shape and conformational changes. Indeed we suggest that AUC will be particularly useful for future studies of MSKs which frequently respond through dimerization and oligomerization events upon ligand binding.

Acknowledgements

We thank Diamond Light Source for B23 beamtime (SM12003, SM12406, SM12310).

Funding

This work was supported by the School of Pharmacy and Biomedical Sciences, University of Central Lancashire and Diamond Light Source [studentship PJX Diamond-UCLan (to C.S.H.)], the University of Leeds and the EU European Drug Initiative for Channels and Transporters [grant number EDICT, 201924 (to P.M.)], and the Biotechnology and Biological Sciences Research Council [grant number BB/D001641/1 (to M.K.P-J. and P.J.F.H.)].

References

1 Fabret, C., Feher, V.A. and Hoch, J.A. (1999) Two-component signal transduction in *Bacillus subtilis*: how one organism sees its world. J. Bacteriol. **181**, 1975–1983 PubMed
2 Dutta, R., Qin, L. and Inouye, M. (1999) Histidine kinases: diversity of domain organization. Mol. Microbiol. **34**, 633–640 CrossRef PubMed
3 Bilwes, A.M., Alex, L.A., Crane, B.R. and Simon, M.I. (1999) Structure of CheA, a signal-transducing histidine kinase. Cell **96**, 131–141 CrossRef PubMed
4 Mascher, T., Helmann, J.D. and Unden, G. (2006) Stimulus perception in bacterial signal-transducing histidine kinases. Microbiol. Mol. Biol. Rev. **70**, 910–938 CrossRef PubMed
5 Potter, C.A., Ward, A., Laguri, C., Williamson, M.P., Henderson, P.J.F. and Phillips-Jones, M.K. (2002) Expression, purification and characterisation of full-length heterologously expressed histidine protein kinase RegB from *Rhodobacter sphaeroides*. J. Mol. Biol. **320**, 201–213 CrossRef PubMed
6 Potter, C.A., Jeong, E.-L., Williamson, M.P., Henderson, P.J.F. and Phillips-Jones, M.K. (2006) Redox-responsive *in vitro* modulation of the signalling state of the isolated PrrB sensor kinase of *Rhodobacter sphaeroides* NCIB 8253. FEBS Lett. **580**, 3206–3210 CrossRef PubMed
7 Oh, J.-Il., Ko, I.-J. and Kaplan, S. (2004) Reconstitution of the *Rhodobacter sphaeroides* cbb_3-PrrBA signal transduction pathway *in vitro*. Biochemistry **43**, 7915–7923 CrossRef PubMed
8 Swem, L.R., Gong, X., Yu, C.-A. and Bauer, C.E. (2006) Identification of a ubiquinone-binding site that affects autophosphorylation of the sensor kinase RegB. J. Biol. Chem. **281**, 6768–6775 CrossRef PubMed
9 Ma, P., Yuille, H.M., Blessie, V., Göhring, N., Iglói, Z, Nishiguchi, K., Nakayama, J., Henderson, P.J.F. and Phillips-Jones, M.K. (2008) Expression, purification and activities of the entire family of intact membrane sensor kinases from *Enterococcus faecalis*. Mol. Membr. Biol. **25**, 449–473 CrossRef PubMed
10 Ward, A., Sanderson, N.M., O'Reilly, J., Rutherford, N.G., Poolman, B. and Henderson, P.J.F. (1999) The amplified expression, identification, purification, assay and properties of histidine-tagged bacterial membrane transport proteins. In Membrane Transport – A Practical Approach (Baldwin, S.A., ed.), pp. 141–166, Blackwell Press, Oxford
11 Ma, P. (2010), Structure–Activity Relationships of Membrane Proteins: The NCS1 Family of Transporters and Sensor Kinases of Two-Component Systems. Ph.D. thesis, University of Leeds, UK
12 Sambrook, J., Fritsch, E.F. and Maniatis, T. (1989) In Molecular Cloning: A Laboratory Manual (Nolan, C., ed.), Cold Spring Harbor Laboratory Press, Cold Spring Harbor, New York
13 Saidijam, M., Psakis, G., Clough, J.L., Meuller, J., Suzuki, S., Hoyle, C.J., Palmer, S.L., Morrison, S.M., Pos, M.K., Essenberg, R.C. et al. (2003) Collection and characterisation of bacterial membrane proteins. FEBS Lett. **555**, 170–175 CrossRef PubMed
14 Seddon, A.M., Curnow, P. and Booth, P.J. (2004) Membrane proteins, lipids and detergents: not just a soap opera. Biochim. Biophys. Acta **1666**, 105–117 CrossRef PubMed
15 Arachea, B.T., Sun, Z., Potente, N., Malik, R., Isailovic, D. and Viola, R.E. (2012) Detergent selection for enhanced extraction of membrane proteins. Protein Exp. Purif. **86**, 12–20 CrossRef
16 Moraes, I., Evans, G., Sanchez-Weatherby, J., Newstead, S. and Stewart, P.D.S. (2014) Membrane protein structure determination – The next generation. Biochim. Biophys. Acta Biomembr. **1838**, 78–87 CrossRef
17 Patching, S.G., Edara, S, Ma, P., Nakayama, J., Hussain, R., Siligardi, G. and Phillips-Jones, M.K. (2012) Interactions of the intact FsrC membrane histidine kinase with its pheromone ligand GBAP revealed through synchrotron radiation circular dichroism. Biochim. Biophys. Acta Biomembr. **1818**, 1595–1602 CrossRef
18 Siligardi, G., Hussain, R., Patching, S.G. and Phillips-Jones, M.K. (2014) Ligand- and drug-binding studies of membrane proteins revealed through circular dichroism spectroscopy. Biochim. Biophys. Acta Biomembr. **1838**, 34–42 CrossRef
19 Marina, A., Waldburger, C.D. and Hendrickson, W.A. (2005) Structure of the entire cytoplasmic portion of a sensor histidine-kinase protein. EMBO J. **24**, 4247–4259 CrossRef PubMed
20 West, A.H. and Stock, A.M. (2001) Histidine kinases and response regulator proteins in two-component signaling systems. Trends Biochem. Sci. **26**, 369–376 CrossRef PubMed

21 Wolanin, P.M., Thomason, P.A. and Stock, J.B. (2002) Histidine protein kinases: key signal transducers outside the animal kingdom. Genom. Biol. **3**, 3013.1–3013.8 CrossRef

22 Rivera-Cancel, G., Ko, W., Tomchick, D.R., Correa, F. and Gardner, K.H. (2014) Full-length structure of a monomeric histidine kinase reveals basis for sensory regulation. Proc. Natl. Acad. Sci. U.S.A. **111**, 17839–17844 CrossRef PubMed

23 Siligardi, G. and Hussain, R. (1998) Biomolecules interactions and competitions by non-immobilised ligand interaction assay by circular dichroism. Enantiomer **3**, 77–87 PubMed

24 Hussain, R., Jávorfi, T. and Siligardi, G. (2012) Spectroscopic analysis: synchrotron radiation circular dichroism. Compr. Chirality **8**, 438–448 CrossRef

25 Siligardi, G., Panaretou, B., Meyer, P., Singh, S., Woolfson, D.N., Piper, P.W., Pearl, L.H. and Prodromou, C. (2002) Regulation of Hsp90 ATPase activity by the co-chaperone Cdc37p/p50cdc37. J. Biol. Chem. **277**, 20151–20159 CrossRef PubMed

26 Martin, S.R., Schilstra, M.J. and Siligardi, G. (2011) Chapter 7: Circular dichroism. In Biophysical Approaches Determining Ligand Binding to Biomolecular Targets, Detection, Measurement and Modelling (Podjarmy, A., Dejaegere, A. and Kieffer, B., eds), pp. 226–246, RSC Publishing CrossRef

27 Hussain, R., Jávorfi, T. and Siligardi, G. (2012) Circular dichroism beamline B23 at the Diamond Light Source. J. Syn. Rad. **19**, 132–135 CrossRef

28 Jávorfi, T., Hussain, R., Myatt, D. and Siligardi, G. (2010) Measuring circular dichroism in a capillary cell using the B23 synchrotron radiation CD beamline at Diamond Light Source. Chirality **22**, E149–E153 CrossRef PubMed

29 Longo, E., De Santis, E., Hussain, R., van Der Walle, C., Casas-finet, J., Uddin, S., dos Santos, A. and Siligardi, G. (2014) The effect of palmitoylation on the conformation and physical stability of a model peptide hormone. Int. J. Pharm. **472**, 156–164 CrossRef PubMed

30 Longo, E., Hussain, R. and Siligardi, G. (2015) Application of circular dichroism and magnetic circular dichroism for assessing biopharmaceuticals formulations photo-stability and small ligands binding properties. Int. J. Pharm. **480**, 84–91 CrossRef PubMed

31 Siligardi, G. and Hussain, R. (2015) CD spectroscopy: an essential tool for quality control of protein folding. Meth. Mol. Biol. **1261**, 255–276 CrossRef

32 Ruzza, P., Siligardi, G., Hussain, R., Marchiani, A., Islami, M., Bubacco, L., Delogu, G., Fabbri, D., Dettori, M.A., Sechi, M. et al. (2014) Ceftriaxone blocks the polymerization of α-synuclein and exerts neuroprotective effects *in vitro*. ACS Chem. Neurosci. **5**, 30–38 CrossRef PubMed

33 Ruzza, P., Hussain, R., Biondi, B., Calderan, A., Tessari, I., Bubacco, L. and Siligardi, G. (2015) Effects of trehalose on thermodynamic properties of alpha-synuclein revealed through synchrotron radiation circular dichroism. Biomolecules **5**, 724–734 CrossRef PubMed

34 Phillips-Jones, M.K., Patching, S.G., Edara, S., Nakayama, J., Hussain, R. and Siligardi, G. (2013) Interactions of the intact FsrC membrane histidine kinase with the tricyclic peptide siamycin I revealed through synchrotron radiation circular dichroism. Phys. Chem. Chem. Phys. **15**, 444–447 CrossRef PubMed

35 Runti, G., del Carmen, L.R.M., Stoilova, T., Hussain, R., Jennions, M., Choudhury, H.G., Benincasa, M., Gennaro, R., Beis, K. and Scocchi, M. (2013) Functional characterization of SbmA, a bacterial inner membrane transporter required for importing the antimicrobial peptide Bac7(1–35). J. Bacteriol. **195**, 5343–5351 CrossRef PubMed

36 Hassan, K.A., Jackson, S., Penesyan, A., Patching, S.G., Tetu, S.G., Eijkelkamp, B.A., Brown, M.H., Henderson, P.J.F. and Paulsen, I.T. (2013) Transcriptomic and biochemical analyses identify a family of chlorhexidine efflux proteins. Proc. Natl. Acad. Sci. U.S.A. **110**, 20254–20259 CrossRef PubMed

37 Marchiani, A., Mammi, S., Siligardi, G., Hussain, R., Tessari, I., Bubacco, L., Delogu, G., Fabbri, D., Dettori, M.A., Sanna, D. et al. (2013) Small molecules interacting with alpha-synuclein: antiaggregating and cytoprotective properties. Amino Acids **45**, 327–338 CrossRef PubMed

38 Hussain, R., Benning, K., Javorfi, T., Longo, E., Rudd, T.R., Pulford, B., Myatt, D. and Siligardi, G. (2015) CDApps: integrated software for experimental planning and data processing at beamline B23, Diamond Light Source. J. Synchr. Rad. **22**, 465–468 CrossRef

39 Sreerama, N. and Woody, R.W. (2004) On the analysis of membrane protein circular dichroism spectra. Protein Sci. **13**, 100–112 CrossRef PubMed

40 Willett, J.W. and Kirby, J.R. (2012) Genetic and biochemical dissection of a HisKA domain identifies residues required exclusively for kinase and phosphatase activities. PLoS Genet. **8**, e1003084 CrossRef PubMed

41 Bettaney, K.E., Sukumar, P., Hussain, R., Siligardi, G., Henderson, P.J.F. and Patching, S.G. (2013) A systematic approach to the amplified expression, functional characterization and purification of inositol transporters from *Bacillus subtilis*. Mol. Membr. Biol. **30**, 3–14 CrossRef PubMed

42 Hagelueken, G., Clarke, B.R., Huang, H., Tuukkanen, A., Danciu, I., Svergun, D.I., Hussain, R., Liu, H., Whitfield, C. and Naismith, J.H. (2015) A coiled-coil domain acts as a molecular ruler to regulate O-antigen chain length in lipopolysaccharide. Nat. Struct. Mol. Biol. **22**, 50–56 CrossRef PubMed

43 Harding, S.E. and Winzor, D.J. (2001) Sedimentation velocity analytical ultracentrifugation. In Protein–Ligand Interactions: Hydrodynamics and Calorimetry (Harding, S.E. and Chowdhry, B.Z., eds), pp. 75–103, Oxford University Press

44 Harding, S.E. and Rowe, A.J. (2010) Insight into protein–protein interactions from analytical ultracentrifugation. Biochem. Soc. Trans. **38**, 901–907 CrossRef PubMed

45 García de la Torre, J. and Harding, S.E. (2013) Hydrodynamic modelling of protein conformation in solution: ELLIPS and HYDRO. Biophys. Rev. **5**, 195–206 CrossRef PubMed

46 Dam, J. and Schuck, P. (2004) Determination of sedimentation coefficient distributions by direct modeling of the sedimentation boundary with Lamm equation solutions. Meth. Enzymol. **384**, 185–212 CrossRef PubMed

47 Harding, S.E., Schuck, P., Abdelhammed, A.S., Adams, G., Kök, M.S. and Morris, G.A. (2011) Extended Fujita approach to the molecular weight distribution of polysaccharides and other polymer systems. Methods **54**, 136–144 CrossRef PubMed

48 Schuck, P., Gillis, R.B., Besong, D., Almutairi, F., Adams, G.G., Rowe, A.J. and Harding, S.E. (2014) SEDFIT-MSTAR: molecular weight and molecular weight distribution analysis of polymers by sedimentation equilibrium in the ultracentrifuge. Analyst **139**, 79–92 CrossRef PubMed

49 Gillis, R.B., Adams, G.G., Heinze, T., Nikolajski, M., Harding, S.E. and Rowe, A.J. (2013) MultiSig: a new high-precision approach to the analysis of complex biomolecular systems. Eur. Biophys. J. **42**, 777–786 CrossRef PubMed

50 Schuck, P. (2003) On the analysis of protein self-association by sedimentation velocity analytical ultracentrifugation. Anal. Biochem. **320**, 104–124 CrossRef PubMed

51 Casey, J.R., Lieberman, D.M. and Reithmeier, R.A.F. (1989) Purification and characterization of Band 3 protein. Meth. Enzymol. **173**, 494–512 CrossRef PubMed

52 Butler, P.J.P. and Tate, C.G. (2005) Correcting for the buoyancy of macromolecules; density increments and apparent partial specific volumes with particular reference to the study of membrane proteins. In Modern Analytical Ultracentrifugation: Techniques and Methods (Scott, D.J., Harding, S.E. and Rowe, A.J., eds), pp. 133–151, Royal Society of Chemistry, Cambridge

53 Cölfen, H., Harding, S.E., Boulter, J.M. and Watts, A. (1996) Hydrodynamic examination of the dimeric cytoplasmic domain of the human erythrocyte anion transporter, band 3. Biophys. J. **71**, 1611–1615 CrossRef PubMed

54 Cölfen, H., Boulter, J.M., Harding, S.E. and Watts, A. (1998) Ultracentrifugation studies on the transmembrane domain of the human erythrocyte anion transporter Band 3 in the detergent C12E8. Eur. Biophys. J. **27**, 651–655 CrossRef PubMed

55 Taylor, A.M., Boulter, J., Harding, S.E., Cölfen, H. and Watts, A. (1999) Hydrodynamic properties of human erythrocyte Band 3 solubilized in reduced Triton X-100. Biophys. J. **76**, 2043–2055 CrossRef PubMed

56 Borges-Walmsley, M.I., Beauchamp, J., Kelly, S.M., Jumel, K., Candlish, D., Harding, S.E., Price, N.C. and Walmsley, A.R. (2003) Identification of oligomerization and drug-binding domains of the membrane fusion protein EmrA. J. Biol. Chem. **278**, 12903–12912 CrossRef PubMed

57 Silkowski, H., Davis, S.J., Barclay, A.N., Rowe, A.J., Harding, S.E. and Byron, O. (1997) Characterisation of the low affinity interaction between rat cell adhesion molecules CD2 and CD48 by analytical ultracentrifugation Eur. Biophys. J. **25**, 455–462

58 Pauleta, S.R., Cooper, A., Nutley, M., Errington, N., Harding, S., Guerlesquin, F., Goodhew, C.F., Moura, I., Moura, J.J.G. and Pettigrew, G.W. (2004) A copper protein and a cytochrome bind at the same site on bacterial cytochrome *c* peroxidase. Biochemistry **43**, 14566–14576 CrossRef PubMed

Received 15 January 2016
doi:10.1042/BST20160023